

Cite this: *New J. Chem.*, 2012, **36**, 371–379

www.rsc.org/njc

PAPER

Synthesis and transport properties of new dendritic core–shell architectures based on hyperbranched polyglycerol with biphenyl-PEG shells†‡

Indah N. Kurniasih,^a Hua Liang,^b Vicki D. Möschwitzer,^a Mohiuddin A. Quadir,^a Michał Radowski,^a Jürgen P. Rabe^b and Rainer Haag^{*a}

Received (in Montpellier, France) 1st June 2011, Accepted 15th July 2011

DOI: 10.1039/c1nj20466a

A new core–shell type of nano-architectures based on hyperbranched polyglycerol (hPG) has been designed by attaching a mono(methoxy)polyethylene glycol (mPEG) shell either directly or through a hydrophobic biphenyl spacer to the hPG scaffold. Alternatively the hPG core was decorated with hydrophobic segments specifically located around the hPG and mPEG as the shell. The constructed structures were compared and contrasted for their ability to solubilize guest molecules of different polarity indices to their corresponding non-solvent for possible drug delivery applications. UV/Vis spectroscopy and Scanning Force Microscopy (SFM) techniques have been used to characterize the host–guest complex. Highly hydrophilic nanocarriers composed of an hPG–mPEG arrangement were found to be very efficient in transporting hydrophilic molecules to an organic environment with almost no encapsulation of the hydrophobic guests. Introduction of biphenyl fragments as hydrophobic spacers between hPG and mPEG, or near the hPG core, substantially increased the hydrophobic guest encapsulation efficiency of the resulting system. The encapsulation and transport properties were found to critically depend on the M_n of hPG, degree of functionalization with hydrophilic and/or hydrophobic fragments and length of mPEG chains, either alone or in combination with each other. SFM images revealed that the size of the nanocarriers is within the range of 10 nm as single particles and 50 nm as aggregates, with the sizes substantially increased upon interaction with the guest species.

Introduction

The use of dendritic macromolecules as drug delivery^{1–11} vehicles is a field of substantial scientific research. However, due to the synthetic complexity to achieve bulk quantities of high generations of dendrimers at low prices,¹² hyperbranched polymers emerged as an alternative to many novel applications of dendritic scaffold.^{8,13–17}

Hyperbranched polyglycerol (hPG) is a highly branched macromolecule that has been prepared from anionic ring-opening polymerization of glycidol (Fig. 1).¹⁸ Extensive research on hPG architectures has been carried out in the last decade by several groups around the globe including ours, revealing multiple unique characteristics of hPG. Initially hPGs with molecular weights of 1–20 kDa were prepared with a degree of polymerization (DP) that can be tailored by the

monomer/initiator ratio to obtain narrow polydispersities (typically < 2.0). It is now possible to develop hPG architectures within the size range of 1 nm to several hundred nanometres. The degree of branching in hPG is only 60% compared to fully branched perfect glycerol dendrimers.^{19,20} So far as biocompatibility issues are concerned, similar, or even improved, profiles have been observed with hPG compared to existing aliphatic polyether polyols, *e.g.*, polysaccharides or polyethylene glycols.^{21–23} Dendritic architectures based on hPG are therefore well-suited for the generation of spherical amphiphilic macromolecules for applications in drug solubilization and delivery.²⁴

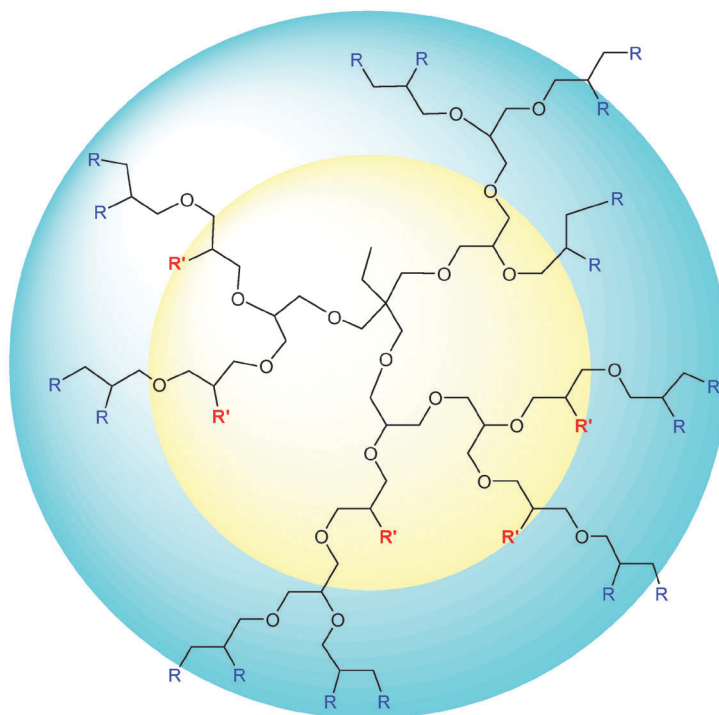
Post-polymerization modification is a powerful gateway to a diversified macromolecular architecture. Incorporation of hydrophilic and/or hydrophobic segments randomly or to a selective location within the preformed hPG scaffold renders the parent molecule with novel and exciting solubility and host–guest interaction properties.^{25,26} One of the primary requisites of such post-modification is the conversion of existing functional groups of the polymer into reactive ones for further chemical changes. Such chemical modification can be easily performed on hPG using classical hydroxyl group chemistry thereby changing the hPG hydroxyl groups namely to azides, alkynes, amines, and to many others.²⁷ Unlike

^a Institute of Chemistry and Biochemistry, Freie Universität Berlin, Takustr. 3, 14195 Berlin, Germany. E-mail: haag@chemie.fu-berlin.de; Fax: +49 30 83853357

^b Department of Physics, Humboldt-Universität zu Berlin, Newtonstr. 15, 12489 Berlin, Germany

† Electronic supplementary information (ESI) available. See DOI: 10.1039/c1nj20466a

‡ This article is part of the themed issue Dendrimers II, guest edited by Jean-Pierre Majoral.



hPG: R,R' = OH

No	Abbreviation	R/R'
1	$\text{hPG}_x(\text{mPEG}_y)_z$	$\text{R} = \left(\text{N} \begin{array}{c} \diagup \text{N} \\ \diagdown \end{array} \text{CH}_2 \text{O-mPEG}_y \right)_z$ or OH
2	$\text{hPG}_{5\text{kDa}}(\text{Biphenyl-mPEG}_7)_z$	$\left(\text{N} \begin{array}{c} \diagup \text{N} \\ \diagdown \end{array} \text{CH}_2 \text{O} \text{---} \text{C}_6\text{H}_4 \text{---} \text{C}_6\text{H}_4 \text{---} \text{O} \text{---} \text{CH}_2 \text{N} \begin{array}{c} \diagup \text{N} \\ \diagdown \end{array} \text{CH}_2 \text{O-mPEG}_7 \right)_z$ or OH
3	$\text{hPG}_{5\text{kDa}}(\text{Biphenyl})_{0.2\text{core}}(\text{mPEG}_7)_{0.6\text{shell}}$	$\text{R} = \left(\text{N} \begin{array}{c} \diagup \text{N} \\ \diagdown \end{array} \text{CH}_2 \text{O-mPEG}_7 \right)_{0.6}$ $\text{R}' = \text{O} \text{---} \text{C}_6\text{H}_4 \text{---} \text{C}_6\text{H}_4$

Fig. 1 Core-shell architectures with the hPG scaffold; [$x = 5$ kDa or 10 kDa; $y = 7, 12, 16, 24, 45$; $z = 0.4, 0.6, 0.9$].

dendrimers hPGs show no distinguishable interior or periphery. Instead they possess two types of hydroxyl functionalities arising from linear and terminal hydroxyl units (Fig. 1). Conceptually, these linear hydroxyl groups are in proximity to the core compared to the terminal ones which are closer to the periphery of the molecule. The so-called “selective chemical differentiation” strategy enables one to selectively and differentially modify these two types of hydroxyl groups to generate core-shell-type architectures within the hPG scaffold.^{19,25,28} To this end, the 1,2-diols of the terminal glycerol units were selectively transformed into the corresponding ketals/acetal in order to distinguish between the interior (close to the focal unit) and periphery (distant from the focal unit) of the macromolecule, which was possible as the remaining linear glycerol units are unaffected by this transformation. A subsequent reaction of the linear units and selective deprotection of 1,2-ketals are generally performed to yield core-functionalized hPGs. The procedure allows selective tailoring of the hPG scaffold to contain hydrophobic substituents (*e.g.* aromatic rings or fluorinated chains) in the interior, thereby modulating the

distribution co-efficient of the generated structure between organic and aqueous phases.

This paper reports the synthetic procedure to generate core-shell architectures of the hPG scaffold containing hydrophilic (PEG) and/or amphiphilic functionality in a random or location-specific manner. The host-guest interaction properties of the synthesized architectures in terms of transport of hydrophilic/hydrophobic guest molecules to corresponding non-compatible media have been compared and contrasted. Different chain lengths of mPEG have been attached to hPG either directly (**1**) or through a biphenyl spacer (**2**) to generate fully hydrophilic or amphiphilic constructs (Fig. 1 and 2). Synthetically such molecules are generated by attaching either mPEGs alone or mPEG pre-coupled with biphenyl spacers to hPG using Cu^I mediated “click chemistry”^{29–31} after conversion of the hPG hydroxyl groups to the corresponding azide functionality. Location specific functionalization of an hPG carrier has been attained by attaching biphenyl rings to the hPG core using a selective “chemical differentiation” strategy, followed by attachment of the PEG chains as the shell to the

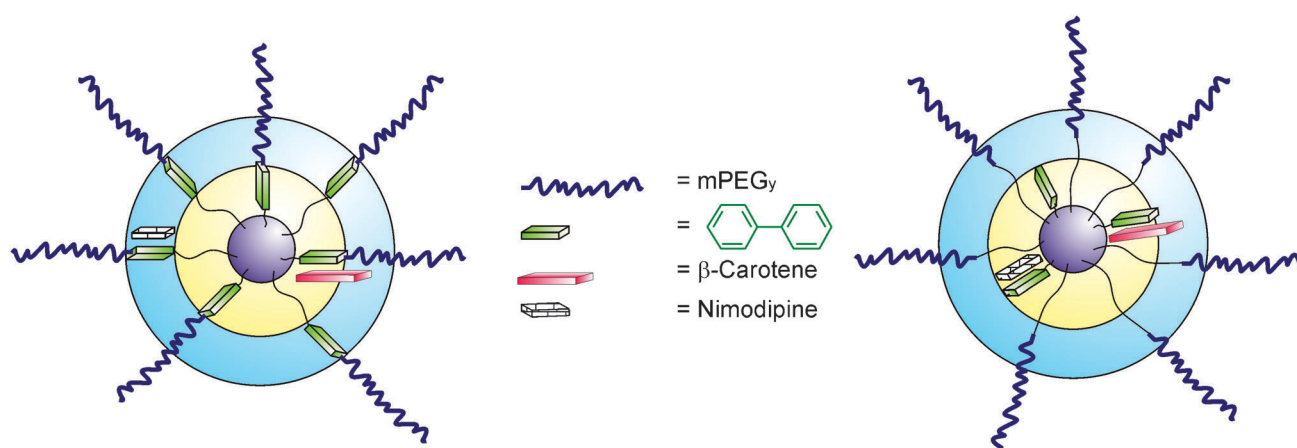


Fig. 2 Model for polymer architectures 2 and 3 with non-polar guest molecules.

peripheral glycerol units (3). The chemical difference between the two categories of constructs lies in the fact that in the case of compounds 1 and 2, the hydrophilic mPEG units or amphiphilic PEG-biphenyl units are randomly distributed throughout the hPG molecule, while for compound 3, the hydrophobic and hydrophilic segments are specifically located within the focal core and the peripheral shell of the hPG respectively. The constructs have been evaluated for their transport capacity as a function of structural diversity, molecular weight of the hPG core, and length of the hydrophilic PEG chain. Efficiency of the synthesized architectures to encapsulate and transport different guest molecules (*i.e.* β -carotene, Congo red, nimodipine and Rose Bengal) to their non-compatible environment has been assessed. The resulting supramolecular assemblies were studied by UV-Vis spectroscopy and SFM measurement.

Experimental part

General strategy for the synthesis of hPG-based core-shell architectures (1–3)

The conceptual scheme of the synthesized polymers and their abbreviations are presented in Fig. 1.

The hPG-based core-shell architecture containing a randomly distributed PEG chain (1) or a biphenyl unit spaced PEG chain (2) was synthesized utilizing Cu^{I} mediated azide-alkyne cycloaddition, widely known as “click chemistry.” The synthesis of construct 2 was carried out first by alkylation of 4,4'-dihydroxyl biphenyl resulting in the bisalkyne-terminated biphenyl derivative. In the following steps, azide terminated mPEG of different lengths was clicked to one of the termini of the biphenyl units. Subsequently, this PEG attached biphenyl moiety was again clicked, this time onto an azide-terminated hPG scaffold. The core-shell system 3 with a biphenyl moiety attached to the hPG core and mPEG units in the periphery (shell) was constructed in a step-wise pattern. Firstly, the biphenyl 4-methyl groups were selectively coupled to the hPG core through etherification by a previously published procedure.²⁵ In the following steps, clickable PEG chains of different lengths were attached to remaining hydroxyl groups *via* the click addition protocol after conversion of these groups to corresponding azide or alkyne groups. The generalized

synthetic scheme for the preparation of the core-shell structures is presented in Fig. 3. For detailed synthetic information and analytical data see ESI.†

Synthesis of core-shell architectures 1: hPG-mPEG system

Alkylation of poly(ethylene glycol) monomethylether (mPEG). 1 eq. of mPEG (7, 12, 16, 24, 45) was dissolved in tetrahydrofuran (THF) and sodium hydride (2 eq.) was added. The mixture was stirred for one hour and propargylbromide (2 eq.) was added dropwise at 0 °C. The reaction mixture was allowed to warm up to room temperature and stirred for 24 h. The crude product was purified by column chromatography

Mesylation of hPG. This reaction was carried out according to the previously published procedure with slight modification. Briefly, hPG (M_n of 5 kDa and 10 kDa) was dissolved in abs. pyridine and mesyl chloride (0.5, 0.7, or 1.0 eq. per OH group depending on the desired degree of functionalization) in abs. pyridine was added dropwise under inert gas. The mixture was stirred at room temperature for 22 h and the crude products were purified by dialysis in acetone to achieve a 40, 60 and 90% functionalized *O*-mesylpolyglycerol.

Azidation of mesylated hPG. Azidation of *O*-mesylpolyglycerol was carried out by dissolving mesylated hPG in dimethylformamide and reacting with sodium azide (4 eq. per OM group). The mixture was stirred at 120 °C for 4 h. After cooling to room temperature the residual sodium azide was removed *via* filtration. The orange filtrate was concentrated *in vacuo* and the crude product was purified by dialysis in chloroform (48 h).

Coupling of alkyne terminated mPEG to hPG. hPG-azide (1 eq. of azide group) and mPEG-alkyne were mixed in THF/water solution (1:1, 20 ml). Next $\text{CuSO}_4 \cdot 5\text{H}_2\text{O}$ (5 mol%) and sodium ascorbate (10 mol%) were added and the mixture was stirred for 24 h at room temperature. The solvent was removed *in vacuo* and the residue was dissolved in methanol. After filtration, the crude product was purified by dialysis in methanol following dialysis in 5% ethylenediamine-tetraacetic (EDTA) acid/water solution to yield the core-shell structure (1).

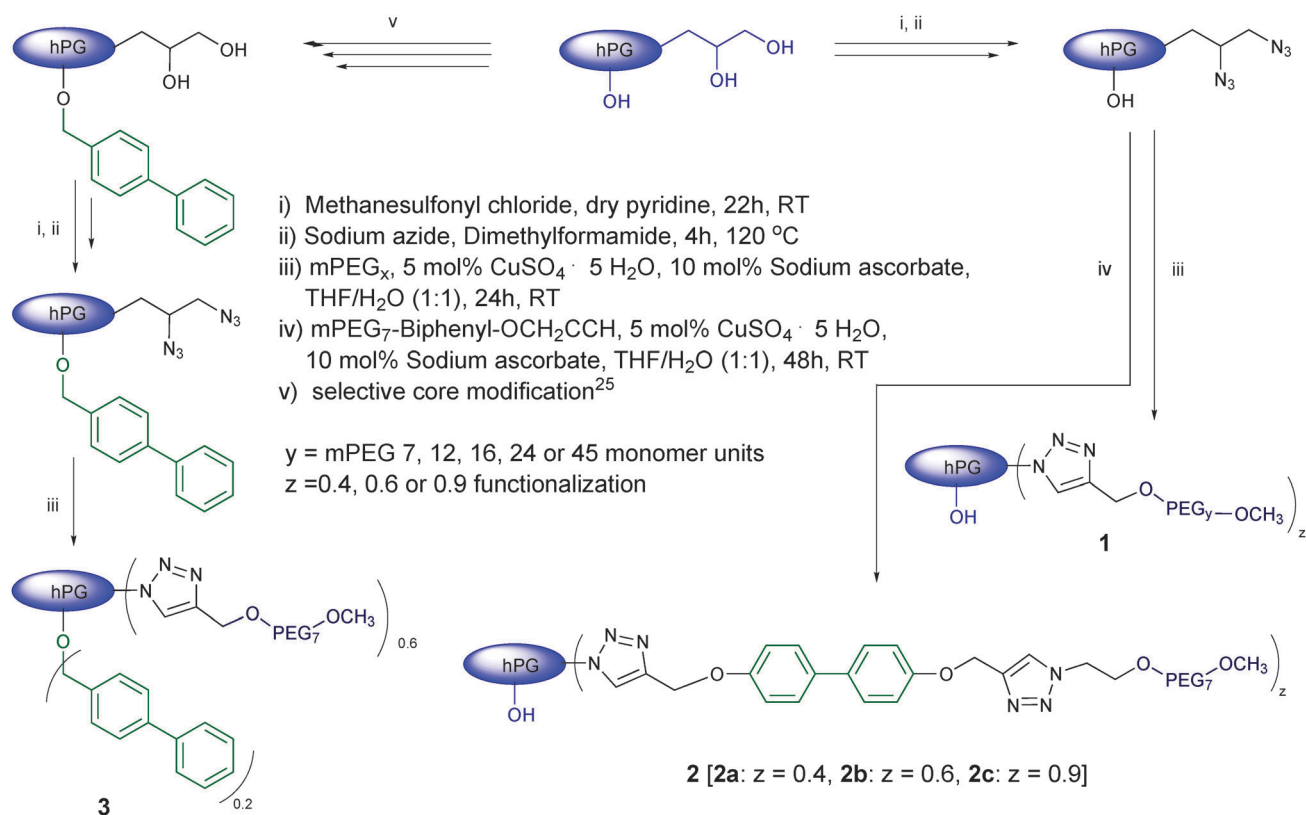


Fig. 3 Synthesis of core-shell architectures (1–3).

Synthesis of core-shell architecture 2: mPEG attached to hPG through a biphenyl spacer

Tosylation of poly(ethylene glycol) monomethylether. mPEG₇ and triethylamine (2.1 eq.) were dissolved in THF and the resulting solution was cooled down to 0 °C. *p*-Toluene sulfonylchloride (1.9 eq.) in THF was added dropwise for 1 h. After stirring for 20 h at room temperature the mixture was filtered to remove the precipitated triethylamine hydrochloride salts. The filtrate was concentrated *in vacuo* and the crude product was purified by column chromatography.

Azidation of *O*-tosyl poly(ethylene glycol) monomethylether. mPEG₇-OTs (1 eq.) was dissolved in dimethylformamide and sodium azide (2 eq.) was added. After 28 h of stirring at room temperature the excess of sodium azide was removed by filtration. Removal of the solvent was done *in vacuo* and the crude product was purified by column chromatography using ethyl acetate as an eluent.

Alkynylation of 4,4'-dihydroxy-biphenyl. To a solution of 4,4'-dihydroxy-biphenyl (1 eq.) in dimethylformamide was added sodium hydride (2 eq.). After stirring for 2 h the solution was cooled down to 0 °C and propargylbromide (2.5 eq.) was added slowly *via* a syringe. The reaction temperature was allowed to rise to room temperature and to run for 49 h. Afterwards, addition of water resulted in precipitation of the product. The mixture was filtered and the product was washed with water to obtain 4,4'-bis(prop-2-ynoxy)biphenyl.

Synthesis of mPEG₇-biphenyl-O-CH₂-C≡CH. 4,4'-Bis(prop-2-ynoxy)biphenyl (3.0 eq.) and mPEG₇-N₃ (1.0 eq.) were mixed with THF. To the resulting suspension in water, CuSO₄·5H₂O (5 mol%), ascorbic acid (10 mol%) and NaOH (10 mol%) were added and the brown mixture was stirred at room temperature for 48 h. After removal of the solvent *in vacuo* THF (20 ml) was added and the mixture was filtered to remove the solid residues. The crude product was purified by column chromatography using chloroform to chloroform/methanol 10:1 as an eluent.

Coupling of alkyne terminated mPEG-biphenyl to hPG. hPG-azide (1 eq. of the azide group) and mPEG₇-biphenyl-O-CH₂-C≡CH (1.3 eq.) were mixed in THF/water solution (1:1, 20 ml). Next CuSO₄·5H₂O (5 mol%) and sodium ascorbate (10 mol%) were added and the mixture was stirred for 24 h at room temperature. The solvent was removed *in vacuo* and the residue was dissolved in methanol. After filtration, the crude product was purified by dialysis in methanol following dialysis in 5% EDTA/water solution.

Synthesis of core-shell architecture 3: hPG with biphenyl units at the core and mPEG at the shell

hPG core functionalized with biphenyl-4-methyl ether group. The reaction was performed according to a previously published procedure.²⁵

Mesylation and azidation of core-functionalized hPG. This reaction was carried out according to the protocol described

for core-shell system **1**, after deprotection of the terminal hydroxyl groups.

Coupling of alkyne terminated mPEG to core-functionalized hPG. Core-functionalized hPG-azide (1 eq. of the azide group) and mPEG-alkyne (1.3 eq.) were mixed in THF/water solution (1:1, 20 ml). Next $\text{CuSO}_4 \cdot 5\text{H}_2\text{O}$ (5 mol%) and sodium ascorbate (10 mol%) were added and the mixture was stirred for 24 h at room temperature. The solvent was removed *in vacuo* and the residue was dissolved in methanol. After filtration, the crude product was purified by dialysis in methanol following dialysis in 5% EDTA/water solution to yield core-shell system **3**.

UV/VIS Spectroscopy

UV/VIS spectra were measured with a *SCINCO* (S-3100) spectrometer (*Jasco* co.) in CHCl_3 or water.

Determination of the transport capacity

The hPG-based core-shell architectures were tested for their capacity to encapsulate and transport guest molecules of varying polarity to non-compatible media. The transport capacity of the carrier systems was determined in a monophasic system with the solvent being either chloroform or water. Polar (Congo red, Rose Bengal) and non-polar (nimodipine, β -carotene) guest molecules (Fig. 4) were used for the transport experiment. For the polar guest molecules chloroform was selected as the non-polar solvent and for the non-polar guest molecules water was used. To the solution of the core-shell architecture (1 g l^{-1}), the guest compound was added as a solid (insoluble in the solution) and the mixtures were rigorously stirred for 16–18 h. After subsequent removal of the non-encapsulated guest molecules *via* a syringe-filter (*Rotilabo*, 13 mm in pore size) the absorption of the solution was measured with UV/VIS spectroscopy and evaluated *via* comparison to a calibration curve.

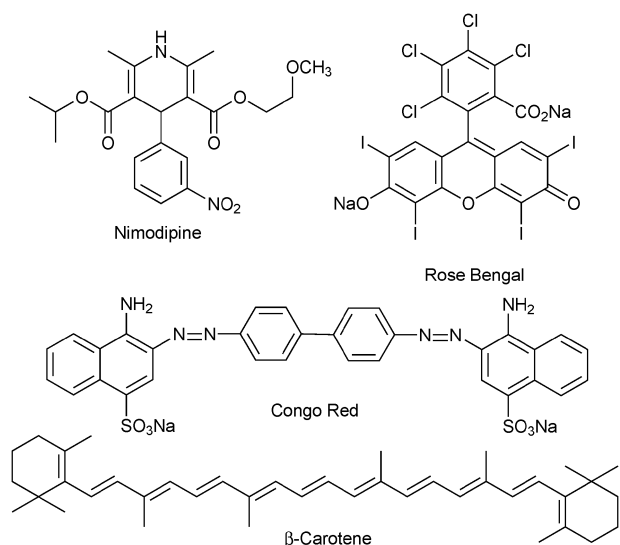


Fig. 4 Structures of polar (Congo red, Rose Bengal) and non-polar (nimodipine, β -carotene) guest molecules.

SFM

A droplet of polymer solution in chloroform and in water was deposited on a freshly cleaved mica surface and spun off after 5 seconds. The surface was dried and imaged by SFM in tapping-mode under ambient conditions, with a Nanoscope 3a (*Veeco*, USA), using silicon cantilevers (*Olympus*, Japan) with a typical resonance frequency of 300 kHz and a spring constant of about 42 N m^{-1} . Both height and phase images were recorded.

Results and discussion

Synthesis of a new core-shell architecture

Three different types of core-shell nanoparticles based on the hPG scaffold have been developed where the constructs varied in terms of specific arrangement of hydrophobic and hydrophilic segments. For both classes of structures, biphenyl moieties and PEG chains represent the hydrophobic and hydrophilic units respectively. While architecture **1** is fully hydrophilic with different chain lengths of mPEG units attached to the hPG scaffold, in core-shell architecture **2**, the hydrophobic and hydrophilic segments are arranged side-by-side and functionalized throughout the hPG scaffold. In core-shell architecture **3**, the hydrophobic biphenyl units are specifically located within the hPG core and the hydrophilic PEG units are located in the shell (Fig. 1). For generating compound **1**, alkyne terminated mPEGs have been attached to azide functionalized hPGs by a straightforward “click reaction”. Architecture **2** was synthesized by bisalkynylation of the biphenyl moiety, followed by coupling to mPEG and attachment of a bisphenyl-mPEG segment to hPG. For generating compound **3**, the biphenyl units are first attached to the core region of hPG by Williamson etherification reaction. Prior to this reaction, the terminal hydroxyl groups were blocked by the formation of acetal and selectively cleaved off after the core-functionalization generating free hydroxyl groups. Conversion of these linear hydroxyl groups to clickable azide or alkyne functionality enabled the immobilization of the alkyne-terminated PEG shell by Cu^{I} assisted click reaction. Both alkyne and azide terminated hPGs were tested with an orthogonally terminated PEG chain to find the best approach. No differences in yields and the functionalization level were observed (yield $\sim 60\%$, functionalization $\sim 90\%$) regardless of azide or alkyne functionalities present in the hPG or in the PEG. The azide groups can be introduced in hPG under ambient reaction conditions in a moderate to high functionalization level. The first step to insert the azide groups is the mesylation of the hPG hydroxyl groups. The extent of mesylation reaction can be stoichiometrically controlled by the amount of applied mesyl chloride. Upon azidation the mesyl groups convert quantitatively to azide groups which can be followed by IR spectroscopy.

The alkyne groups, on the other hand, can also be generated within the hPG scaffold, although a higher degree of alkyne functionalization is difficult to achieve, probably for steric reasons. Additionally densely distributed alkyne functionality over a hPG architecture increases the chance of internal side reactions involving the $\text{C}\equiv\text{C}$ bond. To this end, the route of preferential azidation of hPG has been undertaken to generate

clickable hPG. A series of the substructures have been synthesized following this general protocol by varying the molecular weight of the core, chain length of PEG, and degree of functionalization (ESI[†]).

Transport capacity for hPG–mPEG polymers 1

In order to fully understand the influence of each domain of the macromolecules on the encapsulation efficiency, molecular weight of hPG, the length of the PEG chain, and the level of functionalization were varied to generate a library of substructures of **1** (ESI[†]). hPG–mPEG polymers containing PEG chains of different lengths attached to hPG with no hydrophobic units transported only Congo red and Rose Bengal as guest molecules from water to non-polar solvent (chloroform).

These structures were not able to encapsulate and transport non-polar guest molecules (nimodipine, β -carotene) in water. A similar result has been reported for the unfunctionalized hyperbranched polyglycerol.^{32,33} The reason lies in the fact that these polymers possess a polar hPG core and a highly hydrophilic mPEG periphery that generates a highly polar environment within the molecule. The transport capacity of hPG–mPEG series (hPG core of 5 kDa) for Congo red to the chloroform phase was determined by UV-VIS spectroscopy *via* comparison to calibration curves and is presented in Fig. 5.

With the increase of mPEG length no significant changes in the mg/g transport ratio were observed. Increasing the degree of functionalization on the other hand with mPEGs of different chain lengths caused a generalized reduction of transport capacity probably due to increased steric blockade.

For the polymers with hPG 10 kDa core size, four different PEG lengths (mPEG₇, mPEG₁₂, mPEG₁₆ and mPEG₂₄) were tested as the shell moiety (see ESI[†]). In contrast to molecules with smaller cores the transport ratio initially increases with prolongation of mPEG chains from 7 to 12 glycol units, and then diminishes continuously for longer PEGs with 16 and 24 monomer units. This tendency is best visible for series with 50% level of core functionalization with mPEGs where the transport capacity increases initially from ~ 50 mg g⁻¹ for mPEG₇ to ~ 65 mg g⁻¹ for mPEG₁₂ and then decreases to ~ 45 mg g⁻¹ and ~ 35 mg g⁻¹ for mPEG₁₆ and mPEG₂₄ respectively (ESI[†]).

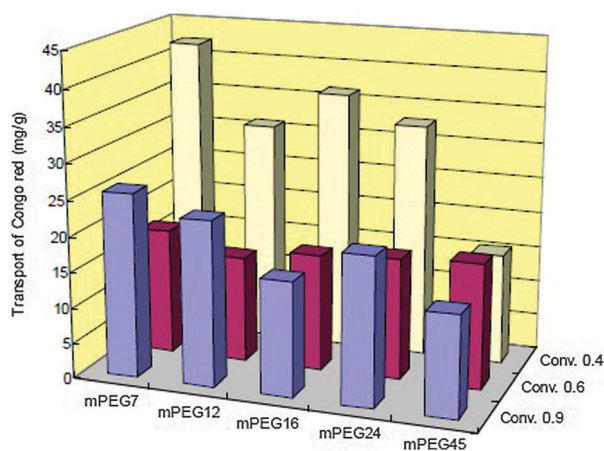


Fig. 5 Transport-structure dependences of polymer with a hPG_{5kDa} core (transport capacities) for Congo red in [mg guest/g polymer].

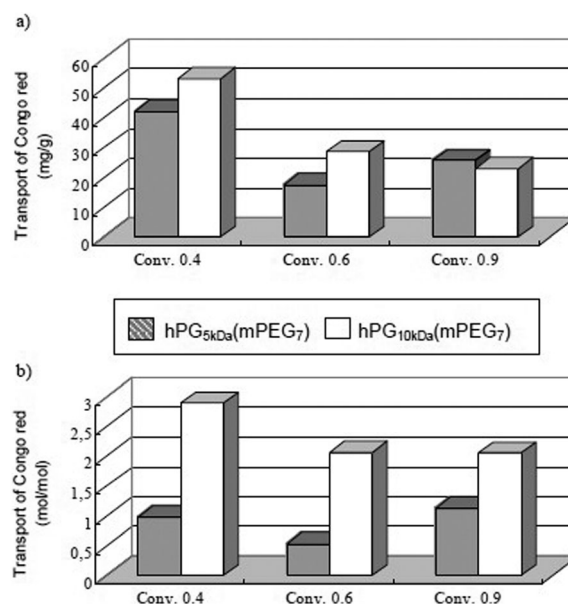


Fig. 6 Transport-structure dependences of core size (hPG_{5kDa}, hPG_{10kDa}) and core functionalization (conversion) demonstrated on polymers with mPEG₇-shells (transport capacities a) in [mg guest/g polymer] and (b) in [mol guest/mol polymer].

The level of core functionalization was found to impart a substantial impact on the transport efficiency of hPG–mPEG polymer series. Increased core functionalization reduces transport capacity both in mg guest/g host or mol guest/mol host level, particularly for the hPG 10 kDa system (Fig. 6). At a high functionalization level of 70% to 90%, the transport capacity remains almost constant or changes irregularly. Modification of the core size increased the mol/mol transport ratio by approximately a factor of three for polymers with a lower functionalization level (40–70%) and by a factor of two for highly functionalized polymers. Considering the higher molecular masses of architectures with a hPG 10 kDa core than those with a hPG 5 kDa core, the change of transport capacity is not substantial in the mg/g ratio. The transport increased only by 20–25% with the increase of the core size for functionalization levels within the range of 40–70% and even slightly decreased for polymers with a 90% functionalized core (Fig. 6). For core–shell architectures with hPG 5 kDa, the effect of functionalization was less prominent than for polymers with a bigger core, and stayed below a factor of two between 90% and 40% core functionalization. The transport result of Rose Bengal encapsulated in a hPG–mPEG polymer was found to be associated with oversaturation phenomena of the carrier molecule with the dye. With increasing amounts of Rose Bengal the encapsulation values rose to a maximum saturation level that led to precipitation of the Rose Bengal–polymer complexes, which were subsequently removed from the solution *via* filtration. Therefore the results of Rose Bengal were not reliable and could not be used for interpretation.

Transport capacity for core–shell architecture 2: mPEG attached to hPG through a biphenyl spacer

Incorporation of a nonpolar element into the core–shell architecture can be used in order to achieve the transport of

non-polar guest molecules in polar solvent.²⁵ The insignificant transport of non-polar guest molecules by the hPG–mPEG systems **1** motivated us to design core–shell architectures where the mPEG units are attached to the hPG core through biphenyl spacers, thereby increasing the amphiphilicity of the molecule. The biphenyl spacer was chosen as a linker because of its interaction with aromatic scaffolds present in different guest molecules (*i.e.* drugs and dyes).

As expected core–shell system **2** solubilized non-polar guest molecule nimodipine in the water phase (Fig. 7). The transport capacity was found to vary directly with increasing levels of functionalization (40 to 90%) of hPG with biphenyl spaced-mPEG units (ESI†). The reported role of the biphenyl spacer to interact with an aromatic π -electron system of nimodipine molecules forming the π – π interaction motif is a major contributing factor for such encapsulation enhancement.²⁵

In the case of β -carotene, the transport capacities of the core–shell system **2** were significantly lower (0.08 mg g^{-1} to 0.50 mg g^{-1}) probably due to the extended structure of β -carotene that is difficult to accommodate within the dendritic scaffold. For Congo red as guest molecules, changes in the encapsulation efficiency of the guest molecule to the host molecule [mg guest/g host] decreased stepwise from 61.76 to 34.81 mg g^{-1} of a polymer with an increasing functionalization level of 40–90% (ESI†).

Transport capacity for core–shell architecture 3: hPG with biphenyl units at the core and mPEG at the shell

Introduction of biphenyl spacers between mPEG and hPG caused a drastic change in the polarity profile of the resulting molecule. In our previous report we have also shown that introduction of a biphenyl fragment into the hPG core *via* a chemical differentiation strategy can change the encapsulated and transport property of hPG. Such molecules with hydrophobic cores and hydrophilic shells were able to solubilize non-polar guest molecules in water.^{25,28} However, this system has the limitation that the conversion of the linear hydroxyl groups of hPG must be lower than 50%, in order to keep the systems soluble in water. Furthermore, the system could not transport polar guest molecules to nonpolar solvent such as chloroform. Combining these two phenomena, we synthesized core–shell architecture **3** by a selective chemical differentiation strategy where the biphenyl units are located near the foci of the hPG scaffold and mPEG units are distributed in the peripheral

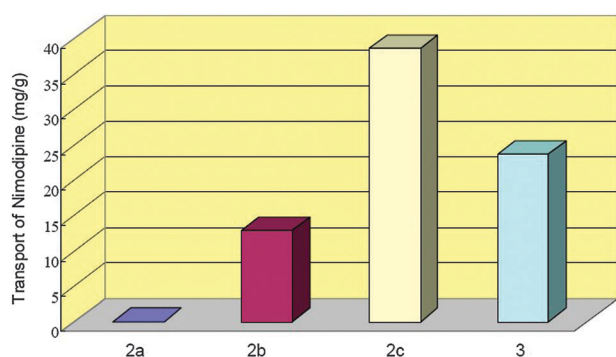


Fig. 7 Transport-structure dependences of Polymer **2a–c** and **3** for nimodipine.

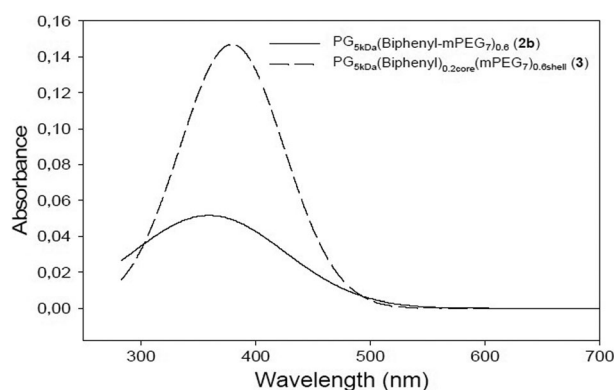


Fig. 8 UV spectra of the complex of nimodipine with polymers **2b** and **3**.

region. It is envisioned that such hybrid structures will include the high non-polar guest transport efficiency of structure **2** and at the same time can carry polar guest molecules to a non-polar environment.

The transport results of nimodipine with such architectures are presented in Fig. 8. The result showed that polymer **3** can transport more nimodipine than core–shell structure **2** at the same level of functionalization with mPEG of equivalent length. Polymer **3**'s transport capacity was also higher than compound **2b**'s which had an even larger number of biphenyl groups (60%). We assumed that the biphenyl spacer at the core facilitated intermolecular aggregation of the hPG scaffolds due to π – π interactions and thereby generated larger aggregates that incorporated more non-polar guest molecules. Furthermore, architecture **3** generated a nonpolar core that increased the hydrophobicity of the system as well as the solubility contribution of nimodipine in the polymer.

For β -carotene as guest molecules, the transport capacity for core–shell architecture **3** was also higher (0.30 mg g^{-1}) than for **2** probably due to increased hydrophobicity and higher propensity of the systems to form aggregates. For Congo red as guest molecules, the transport capacity for compound **3** was lower than for **1** and **2** mostly due to the polarity reduction of the core. However, when Rose Bengal was introduced as the guest molecules to this host polymer, the solubility was higher in **3** than in **2** but lower compared to hPG–mPEG systems with an equivalent level of PEG functionalization.

Host–guest complexes

To reveal the properties of the polymer and the drug/dye complexes (host–guest interaction), scanning force microscopy (SFM) was used. The study was performed by preparing the solution of the polymer in chloroform or water.

Fig. 9 demonstrates hPG₅ kDa(biphenyl)_{0.2core}(mPEG₇)_{0.6shell} (compound **3**) on mica deposited from a chloroform solution of 0.1 mg ml^{-1} . Single round shaped particles with an average size of around 10 nm were detected on the surface. Particles with sizes up to 40 nm were observed (Fig. 9a). Zooming in on one of the particles reveals a double layer structure both in height and phase images: a center core and a surrounding shell (Fig. 9b and c). A height profile across the center of the particle indicated by the dotted line shows the height difference between the central core, the shell, and the substrate

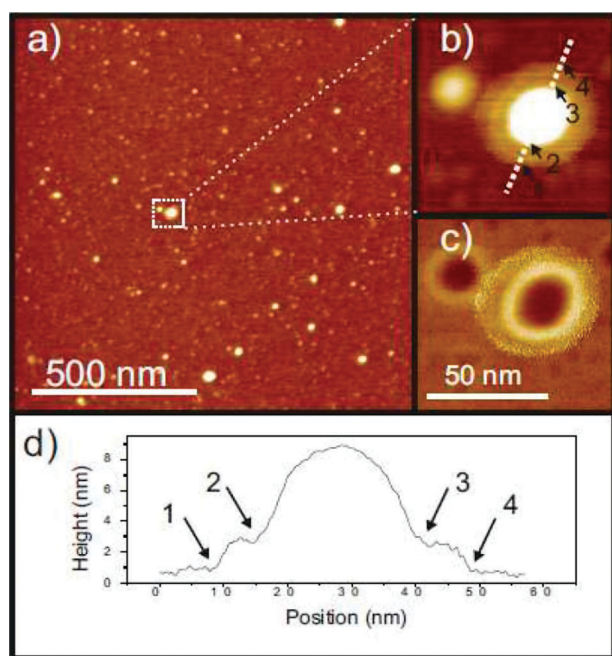


Fig. 9 AFM images of hPG₅ kDa(biphenyl)_{0.2} core(mPEG₇)_{0.6} shell (polymer **3**) in chloroform (0.1 mg ml⁻¹): (a) height image, (b) zoom-in height, (c) phase image, (d) height profile indicated by the dotted line in (b).

respectively (Fig. 9d). Numbers and arrows in the height profile indicate the corresponding positions in the image.

We attribute the single particles to single polymer molecules. The size difference in single particles is attributed to the size distribution of the polymer. The different contrast in both height and phase images may be caused by different chemical components in the core and the shell, which confirms the core-shell structure of the molecule.

In the case of the solution of core-shell structure **3** in water (0.1 mg ml⁻¹), we observed single round shaped small particles of around 10 nm as well as aggregates of around 50 nm (Fig. 10a). Zooming in onto one of the aggregates revealed that the aggregate was formed by single small particles (Fig. 10a and b). The same polymer solution codissolved with nimodipine led to formation of larger aggregates of around 200 nm on the surface (Fig. 10c and d). Again, a higher resolution height image reveals that the aggregates were formed by many small particles.

We attribute the small round shaped particles to single polymer molecules. The aggregates have been shown to form by single molecules through hydrophobic core-core interactions.²⁶ The hydrophilic shell-shell interaction also plays a role in the formation of the aggregates, which is confirmed by the fact that no aggregates formed in a chloroform solution shown in Fig. 9. The presence of hydrophobic organic compounds such as nimodipine seems to enhance the interaction between the molecules, which results in the formation of larger aggregates.

Conclusion

Core-shell type architectures based on hPG have been designed where PEG shells are either directly coupled to hPG or through a biphenyl spacer. The hydrophilic and hydrophobic

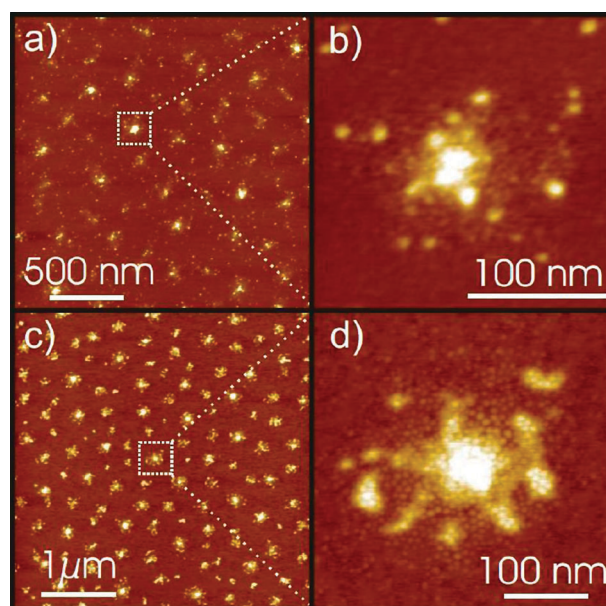


Fig. 10 (a, b) AFM height images of hPG₅ kDa(biphenyl)_{0.2} core(mPEG₇)_{0.6} shell (polymer **3**) in water (0.1 mg ml⁻¹), (c, d) 0.1 mg ml⁻¹ polymer **3** solution with nimodipine.

moieties have also been differently arranged within the hPG scaffold to increase the amphiphilicity of the architecture. Depending on the structural features these nanocarriers were found to encapsulate and transport a wide range of guest molecules. The defined core-shell arrangement in compound **3** showed a significantly higher transport capacity for hydrophobic guest molecules indicating that the stepwise modification of the core and shell leads to more defined systems. In general both nanotransporters **2** and **3** contain aromatic residues and are capable of carrying hydrophobic molecules, which is in clear contrast to hPG-mPEG **1**. The molecular weight of the core, degree of functionalization, and presence of hydrophilic and hydrophobic moieties within the nanocarrier structure were found to critically govern their encapsulation properties. The biocompatibility of the core-shell architectures discussed here is now under investigation for their possible application as drug delivery vehicles.

Acknowledgements

The authors thank Dr Andreas Mohr for the discussion and Meta Mentari for providing hPG-azide. This work was supported by the Bundesministerium für Bildung und Forschung (Nano Future Award for R.H.) and the German Science Foundation (DFG) within the collaborative research center SFB 765.

Notes and references

- 1 J. F. G. A. Jansen, E. M. M. de Brabander-van den Berg and E. W. Meijer, *Science*, 1994, **265**, 1226; M. W. P. L. Baars, R. Kleppinger, M. H. J. Koch, S.-L. Yeu and E. W. Meijer, *Angew. Chem., Int. Ed.*, 2000, **39**, 1285.
- 2 C. C. Lee, J. A. MacKay, J. M. J. Fréchet and F. C. Szoka, *Nat. Biotechnol.*, 2005, **23**, 1517.
- 3 R. Duncan and L. Izzo, *Adv. Drug Delivery Rev.*, 2005, **57**, 2215.
- 4 R. Esfand and D. A. Tomalia, *Drug Discovery Today*, 2001, **6**, 427.

- 5 S. J. Guillaudeu, M. E. Fox, Y. M. Haidar, E. E. Dy, F. C. Szoka and J. M. J. Fréchet, *Bioconjugate Chem.*, 2008, **19**, 461.
- 6 A. W. Bosman, H. M. Janssen and E. W. Meijer, *Chem. Rev.*, 1999, **99**, 1665.
- 7 F. Zeng and S. C. Zimmerman, *Chem. Rev.*, 1997, **97**, 1681.
- 8 C. Gao and D. Yan, *Prog. Polym. Sci.*, 2004, **29**, 183.
- 9 R. Haag, *Angew. Chem., Int. Ed.*, 2004, **43**, 278.
- 10 C. Liu, C. Gao and D. Yan, *Angew. Chem., Int. Ed.*, 2007, **46**, 4128.
- 11 C. Liu, C. Gao and D. Yan, *Macromolecules*, 2006, **39**, 8102.
- 12 C. J. Hawker, *Advanced Computer Simulation Approaches for Soft Matter Science*, Springer, Berlin, 1999, vol. 147, p. 113.
- 13 A. Sunder, J. Heinemann and H. Frey, *Chem.–Eur. J.*, 2000, **6**, 2499.
- 14 R. Haag, *Chem.–Eur. J.*, 2001, **7**, 327.
- 15 N. Karak and S. Maiti, *Dendrimers and Hyperbranched Polymers Synthesis to Applications*, M D Publications Pvt. Ltd, New Delhi, 2008.
- 16 B. Voit and A. Lederer, *Chem. Rev.*, 2009, **109**, 5924.
- 17 Y. Zhou, W. Huang, J. Liu, X. Zhu and D. Yan, *Adv. Mater.*, 2010, **22**, 4567.
- 18 A. Sunder, R. Hanselmann, H. Frey and R. Mülhaupt, *Macromolecules*, 1999, **32**, 4240; A. Sunder, R. Mülhaupt, R. Haag and H. Frey, *Adv. Mater.*, 2000, **12**, 235.
- 19 R. Haag, J.-F. Stumbé, A. Sunder, H. Frey and A. Hebel, *Macromolecules*, 2000, **33**, 8158.
- 20 D. Höltzer, A. Burgath and H. Frey, *Acta Polym.*, 1997, **48**, 30.
- 21 M. Calderon, M. A. Quadir, S. Sharma and R. Haag, *Adv. Mater.*, 2010, **22**, 190.
- 22 D. Howes, R. Wilson and C. T. James, *Food Chem. Toxicol.*, 1998, **36**, 719; R. Wilson, B. J. Van Schie and D. Howes, *Food Chem. Toxicol.*, 1998, **36**, 711.
- 23 R. Haag, A. Sunder and J.-F. Stumbé, *J. Am. Chem. Soc.*, 2000, **122**, 2954.
- 24 R. Haag and F. Kratz, *Angew. Chem., Int. Ed.*, 2006, **45**, 1198.
- 25 H. Türk, A. Shukla, P. C. A. Rodrigues, H. Rehage and R. Haag, *Chem.–Eur. J.*, 2007, **15**, 4187.
- 26 E. Burakowska and R. Haag, *Macromolecules*, 2009, **42**, 5545.
- 27 S. Roller, H. Zhou and R. Haag, *Mol. Diversity*, 2005, **9**, 305–316.
- 28 I. N. Kurniasih, H. Liang, J. P. Rabe and R. Haag, *Macromol. Rapid Commun.*, 2010, **31**, 1516.
- 29 V. V. Rostovtsev, L. G. Green, V. V. Folkin and K. B. Sharpless, *Angew. Chem., Int. Ed.*, 2002, **41**, 2596; C. W. Tornøe, C. Christensen and M. Meldal, *J. Org. Chem.*, 2002, **67**, 3057.
- 30 V. O. Rodinov, V. V. Fokin and M. G. Finn, *Angew. Chem.*, 2005, **117**, 2250; V. O. Rodinov, V. V. Fokin and M. G. Finn, *Angew. Chem., Int. Ed.*, 2005, **44**, 2210.
- 31 V. D. Bock, H. Hiemstra and J. H. v. Maarseveen, *Eur. J. Org. Chem.*, 2006, 51; F. Himo, T. Lovell, R. Hilgraf, V. V. Rostovtsev, L. Noodleman, K. B. Sharpless and V. V. Folkin, *J. Am. Chem. Soc.*, 2005, **127**, 210.
- 32 T. Ooya, J. Lee and K. Park, *J. Controlled Release*, 2003, **93**, 121.
- 33 T. Ooya, J. Lee and K. Park, *Bioconjugate Chem.*, 2004, **15**, 1221.